

(HUANJING KEXUE)

ENVIRONMENTAL SCIENCE

第39卷 第11期

Vol.39 No.11

2018

中国科学院生态环境研究中心 主办

斜学出版社出版



ENVIRONMENTAL SCIENCE

第39卷 第11期 2018年11月15日

目 次

2010~2015年我国水泥工业 NO _x 排放清单及排放特征 ····································
兰州市煨炕污染物排放清单及其对 PM _{2.5} 浓度贡献····································
北京地区气浴胶水浴性组分粒径分布特征 杜翔,赵晋生,苏捷,重群(4858)
郑州市夏、秋季大气颗粒物中水溶性无机离子质量浓度及粒径分布特征 ····································
菏泽市冬季 PM _{2.5} 中二元羧酸类 SOA 的昼夜变化特征 孟静静, 刘晓迪, 侯战方, 李静, 魏本杰, 邢继钊(4876)
我国典型钢铁行业主要工艺环节排放颗粒物源成分谱特征
嘉兴市 2015 年人为源 VOCs 排放清单 · · · · · · · · · · · · · · · · · · ·
上海某石化园区周边区域 VOCs 污染特征及健康风险 ············ 盛涛,陈筱佳,高松,刘启贞,李学峰,伏晴艳(4901)
SBR 工艺城市污水处理厂微生物气溶胶逸散特征 · · · · · · · · · · · · · · · · · · ·
·····································
太湖有色可溶性有机物组成结构对不同水文情景的响应 石玉,周永强,张运林,姚晓龙,黄昌春(4915)
巢湖 2016 年蓝藻水华时空分布及环境驱动力分析
三峡水库低水位运行时干流回水对支流水环境的影响
如米银对胶州湾西北部海区及河口区沉积物反硝化能力和功能基因丰度的影响
澜沧江流域水体悬浮颗粒物8 ¹⁵ N空间差异及成因分析 唐咏春,徐飘,杨正健,张思思,刘德富,纪道斌(4964)
潮白河冲洪积扇典型包气带剖面反硝化强度垂向空间分布规律 耿宏志,郇环,李鸣晓,张莹,从辉,席北斗(4972)
蛤蟆通河流域地下水化学特征及控制因素 张涛,何锦,李敬杰,曹月婷,龚磊,刘金巍,边超,蔡月梅(4981)
典型岩溶地区岩溶泉溶解性碳浓度变化及其通量估算
农村多水塘系统景观结构对非点源污染中氮截留效应的影响 李玉凤,刘红玉,刘军志,娄彩荣,王娟(4999)
城市典型不透水下垫面径流中邻苯二甲酸酯的污染特征····································
不同降雨条件下植被对绿色屋坝径流调羟效益影响
四氧化三铁改性沸石改良低泥对水中磷酸盐的吸附作用 ····································
厌氧条件下可溶性有机质对汞的还原与氧化作用····································
·····································
光助-二茂铁/H ₂ O ₂ 非均相体系降解磺胺二甲基嘧啶
基于同位素技术的短程硝化过程N,O产生途径 ·················· 杨玉兵,杨庆,李洋,周薛扬,李健敏,刘秀红(5051)
基质比对伏氧氨氧化耦合反硝化脱氮除碳的影响 安芳娇,黄剑明,黄利,乔瑞,土瑾,陈永志(5058)
厌氧/好氧 SPNDPR 系统实现低 C/N 城市污水同步脱氮除磷的优化运行
一一一一一一一一一一一一一一一一一一一一一一一一一一一一一一一一一一一一一
方水处理/ SNAD 工艺小试 ····································
盐度对中试厌氧氨氧化脱氮特性的影响及其恢复动力学 ··· 唐佳佳,于德爽,王晓霞,陈光辉,张军,赵红,韩长民(5081)
中试 ANAMMOX-ASBR 处理火电厂脱硫脱硝尾液的抑制及恢复特性 ····································
碳氮比对颗粒污泥 CANON 反应器脱氮性能和N,O释放的冲击影响
污泥性质对微波预处理-厌氧消化的影响及古菌群落结构分析 … 房平, 唐安平, 付兴民, 李伟, 文洋, 佟娟, 魏源送 (5108)
重庆市农地重金属基线值的厘定及其积累特征分析 伍福琳,陈丽,易廷辉,杨志敏,陈玉成(5116)
韩江流域土壤中有机氯农药的特征分布 刘佳, 丁洋, 祁士华, 瞿程凯 (5127)
韩江流域土壤中有机氯农药的特征分布 ····································
纳米零价铁和过氧化钙联合降解土壤淋洗废液的 α -HCH ···································
株洲清水塘上业区周边土壤微生物群洛特征 ··········· 甲丽,李振桦,曾伟氏,余润兰,吴学玲,李交昆,土烁琨(5151)
有机解酸酯任星庆不问城市功能区工壤的分布存征及来源 物态家,何明涓,物婷,尸俊畔,魏臣强(5133)纳米零价铁和过氧化钙联合降解土壤淋洗废液的 α-HCH
生物灰贝钗须处田对小相生长、侬尔尼芯及须系利用的影响
颗粒有机质对水稻辐吸收及转运的影响
施肥对向日葵吸收积累 Cd 的影响
不同水稻品种对重金属的积累特性 林小兵,周利军,王惠明,刘晖,武琳,俞莹,胡敏,何波,周青辉,黄欠如(5198)
芦竹和木本植物间种修复重金属污染土壤 曾鹏,郭朝晖,肖细元,彭驰,黄博(5207)
三峡库区典型河流水-气界面 CO ₂ 通量日变化观测及其影响因素分析 罗佳宸,李思悦 (5217)
生物炭负载氮还田对水稻生长、根系形态及氮素利用的影响
短期放牧对半十早阜地生态系统 CO ₂ 和 N ₂ O
要腊士子和满瓶对真工业产量及农口保排放程度的影响。————————————————————————————————————
復展月刊和催佩四及工不厂里及水口峽肝风烛及即影响 ····································
一大平位及月间内沿面初临汗及压行机化自物(DYOG) 於門門門別九匹成
污水生物处理中抗生素的去除机制及影响因素 张翔宇 李茹莹 季民 (5276)
《环境科学》征订启事(4848) 《环境科学》征稿简则(4990) 信息(5188, 5216, 5236)

北京地区气溶胶水溶性组分粒径分布特征

杜翔1,2,赵普生1*,苏捷1,董群1,3

(1. 中国气象局北京城市气象研究所, 北京 100089; 2. 南开大学环境科学与工程学院, 国家环境保护城市空气颗粒物污染防治重点实验室, 天津 300071; 3. 宁波北仑区气象局, 宁波 315800)

摘要: 2016~2017 年,分别在夏季和冬季在北京城区利用微孔均匀分级采样器(MOUDI-122),采集环境气溶胶,并对其中水溶性离子和水溶性有机物开展了定量分析,对主要水溶性组分质量浓度粒径分布特征,以及季节和不同污染状态下的差异进行了讨论. 结果表明, NH_4^+ 、 NO_3^- 、 SO_4^{2-} 、 K^+ 和冬季 CI^- 主要分布在积聚模态, Mg^{2+} 和 Ca^{2+} 主要分布在粗粒子模态, NH_4^+ 、 NO_3^- 、 SO_4^{2-} 在积聚模态的质量浓度最高,二次离子仍是北京地区 $PM_{2.5}$ 污染的主要组分。 SO_4^{2-} 在夏季浓度较高,而 NO_3^- 、 K^+ 、 CI^- 在冬季明显高于夏季, Mg^{2+} 和 Ca^{2+} 来源较为独立,与气溶胶其他主要组分的相关性较低。夏季 NO_3^- 和 SO_4^{2-} 浓度昼夜差异显著,白天 SO_4^{2-} 浓度水平明显高于夜晚,夜晚 NO_3^- 浓度明显高于白天,且主要表现在积聚模态。污染状况下,二次离子在积聚模态和粗模态浓度增加明显,但在爱根模态中浓度降低。冬季随着污染加重,二次离子液滴模态质量中值粒径明显增大。夏季积聚模态 WSOC 浓度粒径分布峰值粒径明显大于冬季,0.056~0.32 μ m 粒径段 WSOC 在不同污染状态下浓度水平基本一致,在 0.32 μ m 以上区间,污染状态下 WSOC 平均浓度明显高于清洁时段。

关键词:气溶胶;水溶性组分;粒径分布;北京;化学组分

中图分类号: X513 文献标识码: A 文章编号: 0250-3301(2018)11-4858-08 DOI: 10.13227/j. hjkx. 201802146

Size Distributions of Water-soluble Components in Ambient Aerosol of Beijing

DU Xiang^{1,2}, ZHAO Pu-sheng^{1*}, SU Jie¹, DONG Qun^{1,3}

(1. Institute of Urban Meteorology, China Meteorological Administration, Beijing 100089, China; 2. State Environmental Protection Key Laboratory of Urban Ambient Air Particulate Matter Pollution Prevention and Control, College of Environmental Science and Engineering, Nankai University, Tianjin 300071, China; 3. Beilun Bureau of Meteorology, Ningbo 315800, China)

Abstract: A micro-orifice uniform deposit impactor (MOUDI-122) was used to collect ambient aerosol at an urban site in Beijing in both winter and summer from 2016 to 2017. The water-soluble components, including ions and water-soluble organic carbon (WSOC) were analyzed. The characteristics of concentrations and size distributions for water-soluble components under different seasons and pollution conditions were determined. The results showed that NH_4^+ , NO_3^- , SO_4^{2-} , and K^+ in both seasons and Cl^- in winter mainly distributed in the accumulation mode, and Mg^{2+} and Ca^{2+} primarily distributed in the coarse mode. The secondary ions were still the main components of $PM_{2.5}$ in Beijing. The concentrations of SO_4^{2-} were higher in summer, whereas those of NO_3^- , K^+ , and Cl^- were higher in winter. Mg^{2+} and Ca^{2+} had lower correlations with other main components of aerosols, indicating their independent sources. The average size distributions and concentration levels of NO_3^- and SO_4^{2-} exhibited apparent differences between daytime and nighttime in summer. During polluted periods, the concentrations of secondary ions increased in both the accumulation and coarse modes but decreased in the Aitken mode. As pollution levels increased in winter, the mass median diameters of secondary ions in the droplet mode also increased. The WSOC concentration and particle size distribution under accumulation mode in summer were significantly larger than those in winter. The distribution peaks of WSOC in accumulation mode were higher in summer than those in winter. The WSOC in particles of 0.056-0.32 μ m were relatively stable under different pollution levels. However, the WSOC concentration in particles larger than 0.32 μ m during polluted periods was evidently higher than that during clean periods.

Key words; aerosol; water-soluble component; size distribution; Beijing; chemical composition

气溶胶根据其粒径分布特征可归纳为 4 种模态:核模态(3~20 nm)、爱根模态(20~100 nm)、积聚模态(0.1~1 μm)和粗模态(大于1 μm),积聚模态中又有两个亚模态,凝结模态和液滴模态.不同模态气溶胶在理化特征、来源及形成机制方面均有较大差别^[1~4].核模态主要来源为新生成粒子,爱根模态源于燃料燃烧一次排放以及核模态老化,爱根模态通过碰并、凝结进一步增长到积聚模态,已有粒子表面的二次非均相反应也是积聚模态粒子

的重要来源,粗模态主要以扬尘等矿物尘为主.其中积聚模态粒子是 PM_{2.5}质量浓度的主要来源,水溶性物质也主要位于积聚模态,是影响能见度,形成雾-霾重污染的最重要模态.

收稿日期: 2018-02-28; 修订日期: 2018-04-20

基金项目: 国家自然科学基金项目(41675131); 北京市优秀人才培

养资助项目(2014000021223ZK49)

作者简介: 杜翔(1993~), 女, 硕士研究生, 主要研究方向气溶胶

理化特征, E-mail:120445687@qq.com

* 通信作者,E-mail:pszhao@ium.cn

NH₄⁺、NO₃⁻、SO₄² 等二次离子,以及水溶性有 机物(water-soluble organic, WSOC)为气溶胶中主要 水溶性物质, 可以吸收空气中的水分, 使得气溶胶 吸湿增长为液滴, 进而对气溶胶的消光特性、气候 效应以及二次生成机制造成重要影响. 影响气溶胶 散射能力的最主要因素就是气溶胶的粒径分布,而 相对湿度增加造成的吸湿增长会大大提高气溶胶的 散射能力[5~9],特别是相对湿度 > 90% 以上,气溶 胶的散射能力会迅速增加[10,11]. 气溶胶通过吸湿增 长,改变其消光能力的同时,也通过对光线散射直 接影响辐射强迫,同时还通过影响云的形成和降水 过程而影响地气系统的反照率. 此外, 气溶胶吸湿 后,抑制了新粒子形成,为气体-液体-气溶胶非均 相反应提供场所, 并进一步促进 SO, 和 NO, 等在颗 粒物表面的非均相反应, 从而形成一个正反馈机 制,促使更多的硫酸盐和硝酸盐在其表面转化形 成[12~16]. 所以, 了解气溶胶及其主要的水溶性组 分的粒径分布特征及相关影响因素,对于研究气溶 胶生成转化机制,不同粒径气溶胶的吸湿增长能力 以及光学、辐射等尤为重要.

京津冀区域是当前国内气溶胶污染最严重的地区,气溶胶污染引发的雾-霾等重污染及大气低能见度过程引起社会广泛关注. 近些年在北京及周边地区针对 PM_{2.5}污染特征、化学组分及来源等开展了很多相关研究^[17~19],但对于主要化学组分的粒径分布特征,尤其是多粒径区间(不少于十级)特征的研究仍较少,且已有研究主要针对某一时段的水溶性离子^[20~23],对不同季节及不同污染状况下不同组分粒径分布特征的差异缺少讨论.

本课题组在 2013 ~ 2015 年间利用 MOUDI-120 分级采样器,分别在夏季、秋季和冬季在北京城区进行了气溶胶分级样品的系统采集,计算了采样器内部的真实相对湿度,给出了水溶性离子、碳组分(OC、EC)在不同季节不同污染条件下的粒径分布特征,并对不同等级的离子平衡、液态含水量等进行了全面讨论^[24,25].但 MOUDI-120 采样器最小粒径等级只有 0.056 μm,无法给出更细粒径段的分布信息.本次研究利用 MOUDI-122 采样器(最小切割粒径为 0.010 μm)分季节系统采集气溶胶分级样品,在先前研究的基础上进一步增加了爱根模态的信息,并对积聚模态粒径段开展了水溶性有机物组分的分析.基于本研究结果,可以完整获得夏季和冬季不同污染状态下水溶性组分的分布信息,以期为下一步开展不同粒径气溶胶的吸湿增长能力定量

分析提供数据基础,并为二次生成机制、辐射效应 等相关研究提供重要参考.

1 材料与方法

1.1 样品采集和处理

观测点位于北京海淀区三环及四环之间的北京城市气象研究所楼顶(39°94′N,116°30′E), 距地面约36 m, 采样口距离顶楼地面约1.5 m, 采样口周围无各种排气口、通风口. 该观测点周围开阔,无明显污染源,其观测结果可代表北京城区大气污染状况.

选择 MOUDI- 122 型 13 级微孔分级采样器 (micro-orifice uniform deposit impactor, 美国 MSP 公司) 对气溶胶样品进行采集. 采样器流量为 30 $L\cdot min^{-1}$, 校正空气动力学切割粒径分别为 0.01、0.018、0.032、0.056、0.105、0.18、0.32、0.56、1.0、1.8、3.1、6.2、9.9、18 μ m, 每组样品共 13级(大于 18 μ m 及小于 0.01 μ m 的气溶胶粒子不收集).

由于夏季和冬季为北京地区大气污染的代表性季节,所以分别在2016-07-21~2016-07-29及2017-01-14~2017-01-20开展分级采样.每天采集两次,采样时段为08:00~19:00,20:00~次目07:00,单次采样时段为11h,每次采样中间间隔1h,用于滤膜更换和设备清洗.采样器正常采样30min后,使用流量计对流量进行测量,然后根据导出的各级之间的压差变化,计算采样时段内的实际流量.两季均采集7d,每个季节14组样品.具体采样时段及对应的PM_{2.5}平均浓度(Teom1405DF数据)在表1中给出.

MOUDI-122 采样器前十级(0.056~18 μm)采用 Teflon 膜(47 mm, Pall),后三级(0.01~0.056 μm)采用石荚膜(90 mm, Pall),即一组样品包含10 张 Teflon 膜与3 张石荚膜,下面三级使用了特氟龙垫圈来抵消石荚膜的厚度. 样品采集后,滤膜放入冰箱内保存. Teflon 膜性质稳定,可直接使用,石荚膜在使用前在800℃的马弗炉中烘烤3h,用来除去其自身杂质的污染. Teflon 膜性质不易受温湿度影响,可用于质量的精确称重,石荚膜对温湿度则较为敏感,且极易发生碎屑掉落,不能用于称重. 本研究在恒温恒湿条件下(25℃,相对湿度30%)对前十级样品进行了采样前后的滤膜称重.

1.2 样品分析

前 10 级样品, 取整张 Teflon 膜放入称量瓶中,

	表 1	采样时段及采集每组样品时的 PM,	。 平均浓度
--	-----	-------------------	---------------

		夏	季				2	冬季	
样品	采样日期	开始	采样时长	PM _{2.5} 平均浓度	样品	采样日期	开始	采样时长	PM _{2.5} 平均浓度
编号	(年-月-日)	时间	/h	$/\mu g \cdot m^{-3}$	编号	(年-月-日)	时间	/h	$/\mu g \cdot m^{-3}$
X-A	2016-07-21	20:00	11	64. 9	D-A	2017-01-14	08:15	10.75(仪器故障)	15. 7
X-B	2016-07-22	00:80	11	64. 0	D-B	2017-01-14	20:00	11	30. 9
X-C	2016-07-22	20:00	11	114. 8	D-C	2017-01-15	00:80	11	48. 7
X-D	2016-07-23	00:80	11	134. 9	D-D	2017-01-15	20:00	11	80. 2
X-E	2016-07-23	20:00	11	38. 6	D-E	2017-01-16	00:80	11	86. 6
X-F	2016-07-24	00:80	11	98. 2	D-F	2017-01-16	20:00	11	121. 1
X-G	2016-07-25	20:00	11	16. 3	D-G	2017-01-17	00:80	11	142. 6
Х-Н	2016-07-26	00:80	11	22. 8	D-H	2017-01-17	21:40	9.33(仪器故障)	51.6
X-I	2016-07-26	20:00	11	46. 8	D-I	2017-01-18	00:80	11	37. 6
X-J	2016-07-27	00:80	11	70. 7	D-J	2017-01-18	20:00	11	85. 1
X-K	2016-07-27	20:00	11	21. 3	D-K	2017-01-19	00:80	11	24. 1
X-L	2016-07-28	00:80	11	62. 9	D-L	2017-01-19	20:00	11	7.4
X-M	2016-07-28	20:00	11	104. 3	D-M	2017-01-20	00:80	11	22. 1
X-N	2016-07-29	00:80	11	154. 8	D-N	2017-01-20	20:00	11	62. 7

后3级取二分之一石英膜剪碎置于称量瓶中,加入 10 mL 超纯水, 室温下超声 20 min, 为避免超声过 程温度升高导致样品损失, 在超声机中放入冰袋用 于降温. 超声完成后吸取 5 mL 溶液, 经过滤头 (Acrodisc® Syringe Filters)过滤注入专用进样 管内...

将进样管放入 Dionex AS-DV 自动进样器, 进 入离子色谱仪(ICS-1000, DIONEX)进行无机水溶 性离子(Na⁺、NH₄⁺、K⁺、Mg²⁺、Ca²⁺、Cl⁻、NO₃⁻、 SO_4^{2-})的定量分析. 由于实验中采用的各种玻璃仪 器会引入 Na+, 导致其浓度无法准确测出, 且环境 气溶胶中 Na+含量极低, 因此本研究不讨论 Na+的 特征. 离子分析的数据处理、质量控制以及分析的 不确定性分析等,参见文献[24,25].

由于 WSOC 在气溶胶中含量较低, 所以本研究 重点针对 0.056~1.0 μm 的 5 级样品, 取 50 μL 超 声过滤液滴在 0.558 cm² 小石英滤膜上, 干燥后利 用 DRI2001A 型碳分析仪分析各级样品中 WSOC 含量.

2 结果与讨论

经过前期研究发现,利用 MOUDI-120 采样器 采集气溶胶分级样品时,由于气泵抽气导致采样器 内部气压降低, 使得 1.0 µm 以下等级的实际相对 湿度大多低于 40%, 且 1.0 µm 以上粒子吸湿能力 很弱,即采样器工作时采集的气溶胶基本处于干燥 状态, 因此可以不考虑采样时吸湿增长对气溶胶空 气动力学直径的影响[24,25].

2.1 水溶性离子粒径分布季节差异

图 1 和图 2 为夏季和冬季主要水溶性离子平 均粒径分布. 从分布形态上, 能较为明显看出爱 根模态、积聚模态和粗模态. 其中 NH₄ 、NO₃ SO²⁻、K⁺和冬季 Cl⁻主要分布在积聚模态, 夏季 二次离子中可以看到积聚模态中两个亚模态分 布. Mg²⁺和 Ca²⁺则主要分布在粗粒子模态. 此 外,NH₄,K⁺、Mg²⁺在爱根模态范围内分布较为 明显. 从粒径分布上来看, NH₄ 、NO₃ 、SO₄ 在 积聚模态的质量浓度最高, 可见二次离子仍是造 成北京地区 PM25污染的主要组分, 并且冬季 Cl-污染也不容忽视.

夏季和冬季采样期间 PM_{2.5}浓度总平均值分别 为 72. 5 μg·m⁻³ 和 59. 1 μg·m⁻³. 对比冬夏两季的 浓度粒径分布, SO₄² 夏季浓度水平几乎为冬季的 2 倍, 主要原因是夏季光照较强, 温度较高, 可有效 促进 SO_2 向 SO_4^{2-} 的光化学转化. 而冬季 NO_3^{-} 、 K⁺、Cl⁻浓度高于夏季,即此3种离子占PM,5的比 例在冬季明显偏高,主要是冬季化石燃料和生物质 排放增加,同时 SO4- 比例大幅下降所致. 主要组 分浓度粒径分布标准偏差中发现, Mg2+和 Ca2+各 粒径段分布的相对标准偏差整体较低,浓度水平也 较低,表明其来源较为独立,与气溶胶其他主要组 分的相关性较低. 二次离子中, NH₄ 和 SO₄ 在多 数粒径段浓度的相对标准偏差在两个季节基本一 致, 而夏季 NO; 在积聚模态粒径段浓度水平虽然 偏低,但相对标准偏差大大高于冬季,表明夏季 NO: 浓度变化较为剧烈.

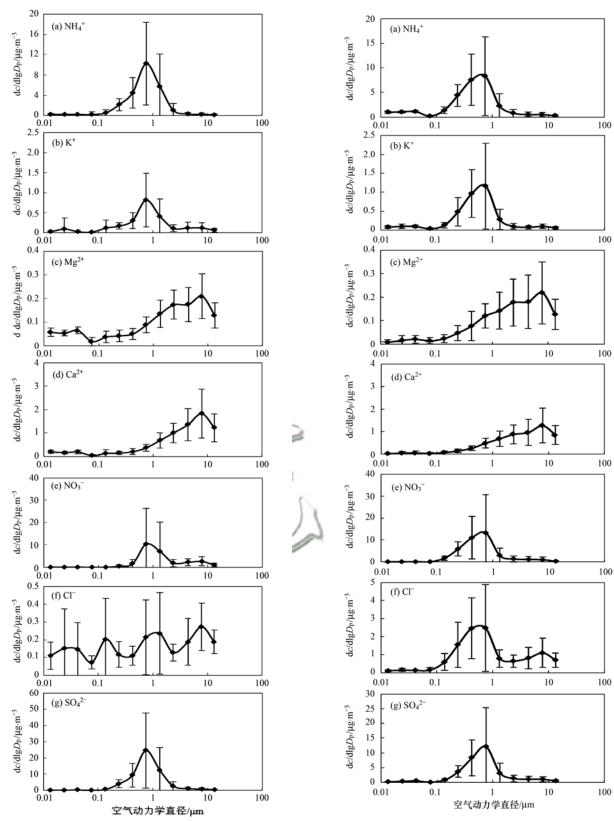


图 1 夏季水溶性离子平均质量浓度分布及其标准偏差

Fig. 1 Average mass concentration distributions and standard deviations of water-soluble ions in summer

2.2 水溶性离子粒径分布昼夜差异 前期研究发现,主要水溶性离子无论在浓

图 2 冬季水溶性离子平均质量浓度分布及其标准偏差

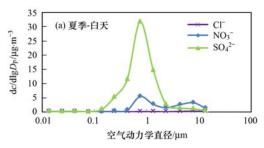
Fig. 2 Average mass concentration distributions and standard deviations of water-soluble ions in winter

度水平还是在分布形态上,昼夜间差异不大^[24,25],本研究中发现冬季水溶离子仍具有类

似特征,而夏季样品中, NO_3^- 和 SO_4^{2-} 昼夜差 异最为显著.其中白天 SO_4^{2-} 浓度水平明显高 于夜晚(图 3),主要原因是此次观测过程白天

整体光照条件较好, SO²⁻ 二次转化较为充分.

与 SO_4^{2-} 相反,夏季夜晚 NO_3^- 浓度明显高于白天,且主要表现在积聚模态,表明夏季夜晚由于相对湿度较高,造成 NO_3^- 生成的非均相二次反应较为显著.



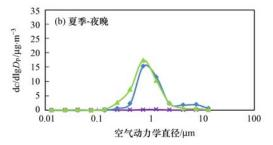


图 3 夏季阴离子平均质量浓度粒径分布

Fig. 3 Average mass concentration distributions of anions in summer

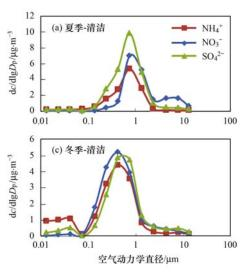
2.3 不同污染条件下水溶性离子分布差异

二次离子是 $PM_{2.5}$ 污染重要组分,也是造成雾霾等低能见度的最主要来源,加之其他一次水溶性离子分布特点较之前没有太大差异,因此本部分主要对二次离子的质量浓度粒径分布特征进行讨论. 此外,各采样时段中,只有采集夏季最后一组样品时 $PM_{2.5}$ 平均浓度达到重污染水平,且仅为 154 μ g·m⁻³,因此将其和其他污染时段合并分析.

图 4 为夏季和冬季污染和清洁条件下主要二次组分的平均粒径分布. 结果显示,污染状况下,3种二次离子总浓度水平(浓度分布线下总面积)均远高于清洁时段. 夏季污染条件下,二次离子中, SO_4^{7} 污染占主导,而冬季污染条件下, SO_4^{6} 和 NO_3^{7} 平均浓度水平相当, NO_3^{7} 浓度最高.

夏季样品 NH₄⁺、SO₄²⁻ 液滴模态的质量中值粒径(MMD) 在 0.75 μm 左右, NO₃⁻ 液滴模态 MMD 在 0.8 μm 左右, 无论污染和清洁时段, 同一离子分布形态基本类似. 而在冬季, 清洁条件下 NH₄⁺ 和 NO₃⁻ 液滴模态 MMD 在 0.45 μm 左右, SO₄²⁻ 在 0.5 μm 左右, 明显小于夏季清洁时段, 到了污染时段, 3 种二次离子的 MMD 明显增加, NH₄⁺ 和 NO₃⁻ 液滴模态 MMD 在 0.7 μm 左右, SO₄²⁻ 在 0.75 μm 左右, 略低于夏季污染时段,表明冬季气溶胶中二次离子随着污染加重,其粒径有明显增大趋势. 此次观测,二次离子分布形态与前期利用 M120 观测类似,不同的是前期观测中,夏季样品随着污染加重,二次离子粒径也有明显增大趋势^[24].

表 2 和表 3 分别给出不同条件下,各粒径范围



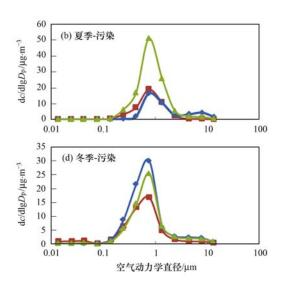


图 4 NH_4^+ 、 NO_3^- 和 SO_4^{2-} 在不同季节不同污染条件下的质量浓度粒径分布

Fig. 4 Mass concentration distributions of NH_4^+ , NO_3^- , and SO_4^{2-} for different seasons and pollution levels

二次离子和总水溶性离子的平均浓度,以及占对应粒径段气溶胶质量的比重(质量分数,下同),由于 $11\sim13$ 级采用 90 mm 石英膜,无法准确称量,所以气溶胶质量浓度只有前十级. 对于夏季样品,粗模态($1.0\sim18~\mu m$)中二次离子,无论是浓度水平还是占气溶胶的比重,污染状态下均高于清洁状态;积聚模态中, NH_4^+ 、 SO_4^{2-} 在污染状态下,平均浓度和占气溶胶比重也整体高于清洁状态,而积聚模态 NO_3^- 在污染状态下,平均浓度略高于清洁时段,占气溶胶比重则低于清洁时段;爱根模态($0.018\sim0.105~\mu m$)中,二次离子污染状态下平均浓度却整体低于清洁状态,其中第十级样品($0.056\sim0.105$

μm)最为明显. 对于冬季样品,粗模态二次离子与夏季类似,污染状态下平均浓度和质量占比均高于清洁状态;积聚模态中,二次离子在污染和清洁状态下占气溶胶的比重基本持平,SO₄-和NO₃-污染下比重略高;爱根模态二次离子在污染状态下的平均浓度与清洁状态下也基本持平,部分粒径略低. 综上,在污染状态下,积聚模态和粗模态中二次离子的质量浓度都会明显增加,然而爱根模态中二次离子的浓度却有所降低,在夏季更为明显,这表明污染过程中,爱根模态中二次离子可能有相当一部分通过碰并、凝结、吸附等过程转化到了积聚模态.

表 2 夏季 NH_4^+ 、 NO_3^- 和 SO_4^{2-} 和总离子平均浓度及其占 PM 比重情况

Table 2	Average mass concentrations and PM	percentages for NH ₄ ⁺ .	$100^{-1} \cdot 100^{-1}$. and total ions in summer

	始汉苗田		质量	量浓度/μg·	m ⁻³			离子占对	対应级别 P	M 比重/%	
项目	粒径范围 /μm	NH ₄ ⁺	SO ₄ ²⁻	NO ₃	总水溶 性离子	气溶胶	NH ₄ ⁺	SO ₄ -	NO ₃	二次离子	总水溶 性离子
	9. 9 ~ 18	0.04	0.08	0. 17	0. 63	4. 69	0. 77	1. 66	3.6	6. 02	13.44
	6. 2 ~ 9. 9	0.03	0.09	0. 34	0.85	4. 58	0.65	1. 99	7.46	10. 11	18. 57
	3. 1 ~ 6. 2	0.06	0. 15	0. 5	1. 17	5.83	1.01	2. 58	8. 57	12. 16	20. 12
	1.8 ~ 3.1	0.09	0. 25	0.35	1.01	4. 52	1.96	5. 58	7. 75	15. 28	22.3
	1 ~ 1. 8	0.74	1. 26	1. 33	3.64	8. 18	9.01	15. 45	16. 32	40. 77	44. 51
	0. 56 ~ 1	1. 35	2. 48	1.76	5. 86	12. 23	11.05	20. 31	14. 42	45. 78	47. 92
夏季-清洁	0. 32 ~ 0. 56	0.67	1. 29	0.31	2.41	6. 69	10. 02	19. 31	4. 58	33. 91	36. 07
9	0. 18 ~ 0. 32	0. 39	0.7	0.12	1. 34	4. 5	8. 73	15. 63	2. 72	27. 08	29. 66
1.1	0. 105 ~ 0. 18	0. 14	0. 15	0.02	0.41	1.54	8. 78	9. 58	1.41	19. 78	26. 67
15	0. 056 ~ 0. 105	0.08	0. 03	0.01	0. 18	0.36	22. 55	8. 87	2. 72	34. 14	50. 98
(a P/1	0. 032 ~ 0. 056	0.06	0.07	0.03	0. 3	/	1. 0	\)		
N3 11	0.018 ~ 0.032	0.06	0.06	0.02	0. 24						
10 P	0.01 ~ 0.018	0.06	0.05	0.02	0. 24						
	9. 9 ~ 18	0.05	0.18	0.45	1. 24	7.95	0.62	2. 24	5.6	8. 46	15.63
1	6. 2 ~ 9. 9	0.1	0.33	0.89	2.04	8.4	1. 14	3. 92	10.61	15. 67	24. 23
	3. 1 ~ 6. 2	0.18	0.65	1.01	2. 58	10.04	1.76	6.46	10.07	18. 29	25. 67
	1.8 ~ 3.1	0.53	1.3	0.67	2. 97	8.62	6. 11	15. 14	7.8	29. 05	34. 45
	1 ~ 1.8	2.77	6. 62	2.7	12.62	19.42	14. 28	34. 08	13. 89	62. 25	64. 96
	0. 56 ~ 1	4. 79	12.88	4. 17	22.44	34. 96	13.69	36. 83	11.92	62. 44	64. 18
夏季-污染	0. 32 ~ 0. 56	1.86	4. 07	0.5	6.68	12.7	14. 65	32. 07	3. 97	50. 69	52. 6
	0. 18 ~ 0. 32	0.8	1.56	0.13	2. 65	6. 34	12.61	24. 55	2.01	39. 17	41. 73
	0. 105 ~ 0. 18	0.13	0. 17	0.02	0.5	1.52	8. 69	11. 13	1.3	21. 12	33.01
	0.056 ~ 0.105	0.01	0.01	0.01	0.06	0.64	1.68	1. 79	1.46	4. 93	9.89
	$0.032 \sim 0.056$	0.05	0.07	0.03	0. 29						
	$0.018 \sim 0.032$	0.06	0.05	0.03	0.35						
	$0.01 \sim 0.018$	0.06	0.07	0.03	0.31						

2.4 WSOC 分布特征

图 5 为 0.056 ~ 1.0 μm 粒径段 WSOC 的平均 浓度粒径分布曲线. 两季节 WSOC 呈现明显不同的 变化趋势, 夏季积聚模态 WSOC 浓度粒径分布峰值 粒径明显大于冬季. 此外, 0.056 ~ 0.32 μm 粒径段 WSOC 在不同污染状态下浓度水平基本一致, 在

0.32 μm 以上区间,污染状态下 WSOC 平均浓度明显高于清洁时段. 在 WSOC 占气溶胶比重方面,随着粒径增大, WSOC 比重也明显增加,在污染状态下 WSOC 在各粒径段的占比均低于清洁状态,这表明污染状态下, WSOC 浓度的增加幅度低于其他主要化学组分.

表 3 冬季 NH_4^+ 、 NO_3^- 和 SO_4^{2-} 及总离子平均浓度及其占 PM 比重情况

Table 3	Average mass concentrations	and PM nercentages	for NH.+ NO	0 502-	and total ions in winter

	始 公 英国		质量	量浓度/μg	m -3			离子占为	付应级别 I	PM 比重/%	
项目	粒径范围 /μm	NH ₄ ⁺	SO ₄ -	NO ₃	总水溶 性离子	气溶胶	NH ₄ ⁺	SO ₄ -	NO ₃	二次离子	总水溶 性离子
	9. 9 ~ 18	0. 03	0.08	0.04	0.48	4. 89	0.71	1. 56	0.85	3. 13	9. 87
	6. 2 ~ 9. 9	0.05	0.1	0.07	0.58	2.93	1.71	3. 54	2. 4	7. 65	19. 96
	3. 1 ~ 6. 2	0.06	0.14	0.14	0.74	3. 23	1.93	4. 19	4. 34	10.46	22. 91
	1.8 ~ 3.1	0.07	0.14	0.15	0.67	3.27	2. 21	4. 37	4. 6	11. 18	20.65
	1 ~ 1.8	0. 21	0.33	0. 27	1. 15	3.44	6. 23	9.66	7. 86	23. 76	33.41
	0. 56 ~ 1	0.9	1. 19	1	3.6	8.03	11. 24	14. 88	12.44	38. 55	44. 87
冬季-清洁	0. 32 ~ 0. 56	1.08	1.18	1. 27	4. 17	9.49	11. 37	12. 48	13.38	37. 23	43.89
	0. 18 ~ 0. 32	0.81	0.65	1.07	3.02	6.65	12. 24	9. 79	16. 15	38. 18	45. 38
	0. 105 ~ 0. 18	0. 29	0.16	0.43	1.09	1.75	16. 7	9. 11	24. 36	50. 18	62. 16
	0.056 ~ 0.105	0.04	0.02	0.04	0.18	0.42	9.66	3.66	8. 92	22. 24	43.47
	$0.032 \sim 0.056$	0. 27	0.13	0.03	0.52						
	0. 018 ~ 0. 032	0. 25	0.09	0.03	0.49						
	$0.01 \sim 0.018$	0. 25	0.06	0.02	0.39						
	9. 9 ~ 18	0.11	0. 21	0. 18	1. 2	7. 16	1. 54	3	2. 57	7. 1	16. 76
	6. 2 ~ 9. 9	0.18	0.38	0.43	1.9	8.87	1.98	4. 24	4. 88	11. 1	21.39
	3. 1 ~ 6. 2	0. 29	0.62	0.73	2.65	11.2	2. 58	5. 5	6. 55	14. 63	23.7
	1.8 ~ 3.1	0.37	0.59	0.66	2. 29	7.83	4,77	7. 55	8. 44	20. 76	29. 23
	1 ~ 1.8	1. 22	1.63	1.56	5. 18	11.89	10. 23	13. 69	13. 11	37. 03	43. 54
	0. 56 ~ 1	4. 22	6.41	7.56	20. 3	38. 33	11. 02	16. 71	19. 73	47. 46	52.96
冬季-污染	0. 32 ~ 0. 56	3. 19	3. 52	5. 25	13.42	26.89	11.88	13. 11	19. 53	44. 52	49. 9
	0. 18 ~ 0. 32	1.58	1. 37	2. 2	5. 87	12.69	12. 46	10. 8	17. 33	40. 6	46. 24
	0. 105 ~ 0. 18	0.36	0. 23	0.38	1. 14	2. 21	16. 15	10. 52	17. 05	43. 71	51.77
	0.056 ~ 0.105	0.05	0.02	0.03	0. 16	0.42	13	3. 94	6. 77	23.71	37.8
/ 1	$0.032 \sim 0.056$	0. 26	0.09	0.05	0.49	,	7/ 8	1 3 9		^	76
3	0.018 ~ 0.032	0. 25	0.06	0.03	0.41		101	1 0	\	(-	6
1.1	0.01 ~ 0.018	0. 23	0. 02	0.03	0. 34	/	6	100	1	~9~	, 1

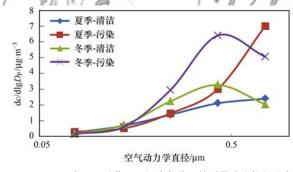


图 5 WSOC 在不同季节不同污染条件下的质量浓度粒径分布 Fig. 5 Mass concentration distributions of WSOC

for different seasons and polluted levels

3 结论

- (1) NH_4^+ 、 NO_3^- 、 SO_4^{2-} 、 K^+ 和冬季 Cl^- 主要分布在积聚模态,但 NH_4^+ 、 K^+ 、 Mg^{2+} 在爱根模态范围内也有明显分布, Mg^{2+} 和 Ca^{2+} 则主要分布在粗粒子模态. NH_4^+ 、 NO_3^- 、 SO_4^{2-} 在积聚模态的质量浓度最高,说明二次离子仍是造成北京地区 $PM_{2.5}$ 污染的主要组分.
 - (2)夏季光照较强,温度较高,利于SO²⁻生

成,冬季 NO_3^- 、 K^+ 、 Cl^- 浓度高于夏季, $SO_4^{2^-}$ 占气溶胶比重明显下降.夏季 NO_3^- 在积聚模态粒径段相对标准偏差远高于冬季,表明夏季 NO_3^- 浓度变化较为剧烈. Mg^{2^+} 和 Ca^{2^+} 各粒径段分布的相对标准偏差及浓度水平整体较低,与气溶胶其他主要组分的相关性较低,来源较为独立.

39 卷

- (3)夏季 NO₃ 和 SO₄ · 浓度粒径分布昼夜差异显著. 白天光照条件较好, SO₄ · 二次转化较为充分, 其浓度水平明显高于夜晚; 而夏季夜晚相对湿度较高, 非均相二次反应显著, 导致夜晚 NO₃ · 浓度明显高于白天, 且主要表现在积聚模态.
- (4)污染状况下,二次离子总浓度水平均远高于清洁时段.夏季污染条件下,二次离子中 SO₄² 污染占主导,冬季污染条件下,SO₄² 和 NO₃ 平均浓度水平相当,NO₃ 浓度略高.夏季样品无论污染和清洁时段,同一离子分布形态基本类似,冬季气溶胶中二次离子随着污染加重,液滴模态 MMD 有明显增大趋势.冬、夏两季污染状态下,积聚模态和粗模态中二次离子质量浓度均明显增加,但爱根

模态中二次离子的浓度却有所降低,夏季更为明显,表明污染过程中,爱根模态中二次离子可能有相当一部分通过碰并、凝结、吸附等过程转化到了积聚模态.

(5)两季 WSOC 呈现不同的变化趋势, 夏季积聚模态 WSOC 浓度粒径分布峰值粒径明显大于冬季. 0.056~0.32 μm 粒径段 WSOC 在不同污染状态下浓度水平基本一致, 0.32 μm 以上区间, 污染状态下 WSOC 平均浓度明显高于清洁时段, 但WSOC 浓度的增加幅度低于其他主要化学组分.

参考文献:

- [1] John W. Size distribution characteristics of aerosols [A]. In: Kulkarni P, Baron P A, Willeke K. Aerosol Measurement: Principles, Techniques, and Applications (3rd ed.) [M]. Hoboken: John Wiley & Sons, Inc, 2011. 41-54.
- [2] Ramachandran G, Cooper D W. Size distribution data analysis and presentation [A]. In: Kulkarni P, Baron P A, Willeke K. Aerosol Measurement: Principles, Techniques, and Applications (3rd ed.) [M]. Hoboken: John Wiley & Sons, Inc, 2011. 479-506.
- [3] Seinfeld J H, Pandis S N. Atmospheric Chemistry and Physics: From Air Pollution to Climate Change (3rd ed.) [M]. Hoboken: John Wiley & Sons, 2016. 325-361.
- [4] Wu Z J, Hu M, Lin P, et al. Particle number size distribution in the urban atmosphere of Beijing, China [J]. Atmospheric Environment, 2008, 42(34): 7967-7980.
- Environment, 2008, 42(34): 7967-7980.

 [5] Tang I N. Chemical and size effects of hygroscopic aerosols on light scattering coefficients [J]. Journal of Geophysical Research, 1996, 101(D14): 19245-19250.
- [6] Eichler H, Cheng Y F, Birmili W, et al. Hygroscopic properties and extinction of aerosol particles at ambient relative humidity in South-Eastern China [J]. Atmospheric Environment, 2008, 42 (25): 6321-6334.
- [7] Pan X L, Yan P, Tang J, et al. Observational study of influence of aerosol hygroscopic growth on scattering coefficient over rural area near Beijing mega-city [J]. Atmospheric Chemistry and Physics, 2009, 9(19): 7519-7530.
- [8] Liu X G, Gu J W, Li Y P, et al. Increase of aerosol scattering by hygroscopic growth; observation, modeling, and implications on visibility [J]. Atmospheric Research, 2013, 132-133: 91-101.
- [9] Chen J, Zhao C S, Ma N, et al. Aerosol hygroscopicity parameter derived from the light scattering enhancement factor measurements in the North China Plain [J]. Atmospheric Chemistry and Physics, 2014, 14(15); 8105-8118.
- [10] Liu P F, Zhao C S, Göbel T, et al. Hygroscopic properties of aerosol particles at high relative humidity and their diurnal variations in the North China Plain [J]. Atmospheric Chemistry and Physics, 2011, 11(7): 3479-3494.
- [11] Chen J, Zhao C S, Ma N, et al. A parameterization of low visibilities for hazy days in the North China Plain [J]. Atmospheric Chemistry and Physics, 2012, 12 (11): 4935-

- 4950
- [12] McMurry P H, Wilson J C. Droplet phase (Heterogeneous) and gas phase (homogeneous) contributions to secondary ambient aerosol formation as functions of relative humidity[J]. Journal of Geophysical Research, 1983, 88(C9): 5101-5108.
- [13] Dentener F J, Carmichael G R, Zhang Y, et al. Role of mineral aerosol as a reactive surface in the global troposphere [J]. Journal of Geophysical Research, 1996, 101 (D17): 22869-22889.
- [14] Ravishankara A R. Heterogeneous and multiphase chemistry in the troposphere [J]. Science, 1997, 276(5315): 1058-1065.
- [15] Kolb C E, Cox R A, Abbatt J P D, et al. An overview of current issues in the uptake of atmospheric trace gases by aerosols and clouds [J]. Atmospheric Chemistry and Physics, 2010, 10 (21): 10561-10605.
- [16] Li W J, Li P R, Sun G D, et al. Cloud residues and interstitial aerosols from non-precipitating clouds over an industrial and urban area in northern China [J]. Atmospheric Environment, 2011, 45(15): 2488-2495.
- [17] He K B, Yang F M, Ma Y L, et al. The characteristics of PM_{2.5} in Beijing, China [J]. Atmospheric Environment, 2001, 35 (29): 4959-4970.
- [18] Ianniello A, Spataro F, Esposito G, et al. Chemical characteristics of inorganic ammonium salts in PM_{2.5} in the atmosphere of Beijing (China) [J]. Atmospheric Chemistry and Physics, 2011, 11(21): 10803-10822.
- [19] Zhao P S, Dong F, He D, et al. Characteristics of concentrations and chemical compositions for PM_{2.5} in the region of Beijing, Tianjin, and Hebei, China [J]. Atmospheric Chemistry and Physics, 2013, 13(9): 4631-4644.
- [20] Yao X H, Lau A P S, Fang M, et al. Size distributions and formation of ionic species in atmospheric particulate pollutants in Beijing, China: 1—inorganic ions [J]. Atmospheric Environment, 2003, 37(21): 2991-3000.
- [21] Guo S, Hu M, Wang Z B, et al. Size-resolved aerosol water-soluble ionic compositions in the summer of Beijing: implication of regional secondary formation [J]. Atmospheric Chemistry and Physics, 2010, 10(3): 947-959.
- [22] Wang X F, Wang T, Pathak R K, et al. Size distributions of aerosol sulfates and nitrates in Beijing during the 2008 Olympic Games: impacts of pollution control measures and regional transport [J]. Advances in Atmospheric Sciences, 2013, 30 (2): 341-353.
- [23] 胡敏, 赵云良, 何凌燕, 等. 北京冬、夏季颗粒物及其离子成分质量浓度谱分布[J]. 环境科学, 2005, **26**(4): 1-6. Hu M, Zhao Y L, He L Y, *et al.* Mass size distribution of Beijing particulate matters and its inorganic water-soluble ions in winter and summer[J]. Environmental Science, 2005, **26**(4): 1-6.
- [24] Zhao P S, Chen Y N, Su J. Size-resolved carbonaceous components and water-soluble ions measurements of ambient aerosol in Beijing[J]. Journal of Environmental Sciences, 2017, 54: 298-313.
- [25] Su J, Zhao P S, Dong Q. Chemical compositions and liquid water content of size-resolved aerosol in Beijing[J]. Aerosol and Air Quality Research, 2018, 18(3): 680-692.

HUANJING KEXUE

Environmental Science (monthly)

Vol. 39 No. 11 Nov. 15, 2018

CONTENTS

Emissions Inventory and Characteristics of NO_{x} from Cement Industry		
Emissions Inventory of Smoldering Chinese Kangs and Their Contribution to PM _{2.5} Pollution in Lanzhou City		
Size Distributions of Water-soluble Components in Ambient Aerosol of Beijing		
Size Distribution Characteristics of Water-Soluble Inorganic Ions During Summer and Autumn in Zhengzhou		
Diurnal Variation of Dicarboxylic Acids and Related SOA in PM _{2.5} from Heze City in Winter		
Chemical Source Profiles of PM Emitted from the Main Processes of the Iron and Steel Industry in China		
VOCs Emission Inventory of Anthropogenic Sources in Jiaxing		
Pollution Characteristics and Health Risk Assessment of VOCs in Areas Surrounding a Petrochemical Park in Shanghai		
Characteristics of Bioaerosols Emitted from WWTP with SBR Treatment Process		
Response of Chromophoric Dissolved Organic Matter Composition to Different Hydrological Scenarios in Large Eutrophic Lake Tail	nu ··· SHI Yu, ZHOU Yong-qiang, ZHANG Yun-lin, et al.	(4915)
Spatial and Temporal Dynamics of Floating Algal Blooms in Lake Chaohu in 2016 and Their Environmental Drivers		
Dynamic Changes of Nitrogen-Transforming and Phosphorus-Accumulating Bacteria Along with the Formation of Cyanobacterial Bloom	ooms	
		(4938)
$Impact \ of \ Mainstream \ Backwater \ on \ the \ Water \ Environment \ of \ the \ Tributaries \ of \ the \ Three \ Gorges \ Reservoir \ at \ Low \ Water \ Level \ \cdot \ Annual \ Annu$,
		(4946)
Effect of Silver Nanoparticles on Denitrification and Functional Gene Abundances of Sediment in Dagu River Estuary and Northwe	st of Jiaozhou Bay	(4056)
Spatial Difference and Causes Analysis of the δ ¹⁵ N of Suspended Particulate Matter in the Lancang River Basin	0 1	
Vertical Spatial Distribution of Denitrification Intensity in the Vadose Zone of Typical Sections of Chaobai River Alluvial Fan		
Major Ionic Features and Possible Controls in the Groundwater in the Hamatong River Basin		
Concentration Variations and Flux Estimation of Dissolved Carbon in Karst Spring of a Typical Karst Area		
Effect of Different Multi-pond Network Landscape Structures on Nitrogen Retention Over Agricultural Watersheds		
Characteristics of Phthalic Acid Esters Pollution in Urban Surface Runoff in Shanghai, China		
Impacts of Vegetation on Hydrological Performances of Green Roofs Under Different Rainfall Conditions	-	
Adsorption of Phosphate from Aqueous Solutions on Sediments Amended with Magnetite-Modified Zeolite		
Reduction and Oxidation of Mercury by Dissolved Organic Matter Under Anaerobic Conditions		
Photo-assisted Degradation of Sulfamethazine by Ferrocene-catalyzed Heterogeneous Fenton-like System		
$\mathrm{N}_2\mathrm{O}$ Production Pathways in Partial Nitrification Based on Isotope Technology \cdots		
Effect of Substrate Ratio on Removal of Nitrogen and Carbon Using Anaerobic Ammonium Oxidation and Denitrification		(5058)
Simultaneous Nitrogen and Phosphorus Removal Characteristics of An Anaerobic/Aerobic Operated SPNDPR System Treating Low	C/N Urban Sewage	
Lab-scale SNAD Process in Wastewater Treatment Plant		(5074)
Effect of Salinity on Nitrogen Removal Performance of a Pilot-scale Anaerobic Ammonia Oxidation Process and Its Recovery Kinet	ics ·····	
		(5081)
Suppression and Recovery Characteristics of Pilot-scale ANAMMOX-ASBR System Treating Desulfurization and Denitrification Tail	lings from Thermal Power Plant · · · · · · · · · · · · · · · · · · ·	
		(5090)
$Impact\ of\ C/N\ Ratio\ on\ Nitrogen\ Removal\ Performance\ and\ N_2O\ Release\ of\ Granular\ Sludge\ CANON\ Reactor\ \cdots$		
I COLLOL CONTROL A LUDY COLLABOR DE LA LABOR COLLABOR		
Impacts of Sludge Characteristics on Anaerobic Digestion with Microwave Pretreatment and Archaeal Community Structure Analysis	s ······ FANG Ping, TANG An-ping, FU Xing-min, et al.	(5108)
Determination of Heavy Metal Baseline Values and Analysis of Its Accumulation Characteristics in Agricultural Land in Chongqing	s ······· FANG Ping, TANG An-ping, FU Xing-min, et al. g ······ WU Fu-lin, CHEN Li, YI Ting-hui, et al.	(5108) (5116)
Determination of Heavy Metal Baseline Values and Analysis of Its Accumulation Characteristics in Agricultural Land in Chongqing Characteristics of Organochlorine Pesticides (OCPs) in Soil Samples of Hanjiang River Basin, Southeast China	s ······ FANG Ping, TANG An-ping, FU Xing-min, et al. WU Fu-lin, CHEN Li, YI Ting-hui, et al. LIU Jia, DING Yang, QI Shi-hua, et al.	(5108) (5116) (5127)
Determination of Heavy Metal Baseline Values and Analysis of Its Accumulation Characteristics in Agricultural Land in Chongqing Characteristics of Organochlorine Pesticides (OCPs) in Soil Samples of Hanjiang River Basin, Southeast China Occurrence and Distribution of the Organophosphate Esters in Soils of Mixed-land Use Area in Chongqing City	s ······· FANG Ping, TANG An-ping, FU Xing-min, et al. WU Fu-lin, CHEN Li, YI Ting-hui, et al. LIU Jia, DING Yang, QI Shi-hua, et al. YANG Zhi-hao, HE Ming-jing, YANG Ting, et al.	(5108) (5116) (5127) (5135)
Determination of Heavy Metal Baseline Values and Analysis of Its Accumulation Characteristics in Agricultural Land in Chongqing Characteristics of Organochlorine Pesticides (OCPs) in Soil Samples of Hanjiang River Basin, Southeast China Occurrence and Distribution of the Organophosphate Esters in Soils of Mixed-land Use Area in Chongqing City Degradation of α -HCH in Soil Washing Solutions with nZVI and CaO $_2$	s ······ FANG Ping, TANG An-ping, FU Xing-min, et al. WU Fu-lin, CHEN Li, YI Ting-hui, et al. LIU Jia, DING Yang, QI Shi-hua, et al. YANG Zhi-hao, HE Ming-jing, YANG Ting, et al. YAO Jing-bo, ZHOU Jie, WANG Ming-xin, et al.	(5108) (5116) (5127) (5135) (5142)
Determination of Heavy Metal Baseline Values and Analysis of Its Accumulation Characteristics in Agricultural Land in Chongqing Characteristics of Organochlorine Pesticides (OCPs) in Soil Samples of Hanjiang River Basin, Southeast China Occurrence and Distribution of the Organophosphate Esters in Soils of Mixed-land Use Area in Chongqing City Degradation of α -HCH in Soil Washing Solutions with nZVI and CaO ₂ Microbial Communities in Soils of Qingshuitang Industrial District in Zhuzhou	s FANG Ping, TANG An-ping, FU Xing-min, et al. g	(5108) (5116) (5127) (5135) (5142) (5151)
Determination of Heavy Metal Baseline Values and Analysis of Its Accumulation Characteristics in Agricultural Land in Chongqing Characteristics of Organochlorine Pesticides (OCPs) in Soil Samples of Hanjiang River Basin, Southeast China Occurrence and Distribution of the Organophosphate Esters in Soils of Mixed-land Use Area in Chongqing City Degradation of α -HCH in Soil Washing Solutions with nZVI and CaO $_2$	s FANG Ping, TANG An-ping, FU Xing-min, et al. g	(5108) (5116) (5127) (5135) (5142) (5151)
Determination of Heavy Metal Baseline Values and Analysis of Its Accumulation Characteristics in Agricultural Land in Chongqing Characteristics of Organochlorine Pesticides (OCPs) in Soil Samples of Hanjiang River Basin, Southeast China	s FANG Ping, TANG An-ping, FU Xing-min, et al. g	(5108) (5116) (5127) (5135) (5142) (5151) (5163) (5170)
Determination of Heavy Metal Baseline Values and Analysis of Its Accumulation Characteristics in Agricultural Land in Chongqing Characteristics of Organochlorine Pesticides (OCPs) in Soil Samples of Hanjiang River Basin, Southeast China	s FANG Ping, TANG An-ping, FU Xing-min, et al. WU Fu-lin, CHEN Li, YI Ting-hui, et al. LIU Jia, DING Yang, QI Shi-hua, et al. YANG Zhi-hao, HE Ming-jing, YANG Ting, et al. YAO Jing-bo, ZHOU Jie, WANG Ming-xin, et al. SHEN Li, LI Zhen-hua, ZENG Wei-min, et al. WANG Dan-dan, YANG Ze-ping, ZHAO Yuan, et al. YU Ying-liang, WANG Yue-man, HOU Peng-fu, et al. GUO Yi-xuan, ZHAO Xiu-lan	(5108) (5116) (5127) (5135) (5142) (5151) (5163) (5170) (5180)
Determination of Heavy Metal Baseline Values and Analysis of Its Accumulation Characteristics in Agricultural Land in Chongqing Characteristics of Organochlorine Pesticides (OCPs) in Soil Samples of Hanjiang River Basin, Southeast China Occurrence and Distribution of the Organophosphate Esters in Soils of Mixed-land Use Area in Chongqing City Degradation of α -HCH in Soil Washing Solutions with nZVI and CaO $_2$ Microbial Communities in Soils of Qingshuitang Industrial District in Zhuzhou Effect of Biochar Addition on the Diversity and Interaction of Rhizosphere Fungi in Manure-fertilized Soil Effects of Returning Nitrogen by Biochar Loading on Paddy Growth, Root Morphology, and Nitrogen Use Efficiency Effect of Particulate Organic Matter on Cadmium Uptake and Transport in Rice Effect of Fertilizers on Cadmium Uptake and Accumulation by Sunflowers	s FANG Ping, TANG An-ping, FU Xing-min, et al. WU Fu-lin, CHEN Li, YI Ting-hui, et al. LIU Jia, DING Yang, QI Shi-hua, et al. YANG Zhi-hao, HE Ming-jing, YANG Ting, et al. YAO Jing-bo, ZHOU Jie, WANG Ming-xin, et al. SHEN Li, LI Zhen-hua, ZENG Wei-min, et al. WANG Dan-dan, YANG Ze-ping, ZHAO Yuan, et al. YU Ying-liang, WANG Yue-man, HOU Peng-fu, et al. GUO Yi-xuan, ZHAO Xiu-lan CAO Liu, YANG Jun-xing, GUO Jin-jun, et al.	(5108) (5116) (5127) (5135) (5142) (5151) (5163) (5170) (5180) (5189)
Determination of Heavy Metal Baseline Values and Analysis of Its Accumulation Characteristics in Agricultural Land in Chongqing Characteristics of Organochlorine Pesticides (OCPs) in Soil Samples of Hanjiang River Basin, Southeast China Occurrence and Distribution of the Organophosphate Esters in Soils of Mixed-land Use Area in Chongqing City Degradation of α -HCH in Soil Washing Solutions with nZVI and CaO ₂	s FANG Ping, TANG An-ping, FU Xing-min, et al. WU Fu-lin, CHEN Li, YI Ting-hui, et al. LIU Jia, DING Yang, QI Shi-hua, et al. YANG Zhi-hao, HE Ming-jing, YANG Ting, et al. YAO Jing-bo, ZHOU Jie, WANG Ming-xin, et al. SHEN Li, LI Zhen-hua, ZENG Wei-min, et al. WANG Dan-dan, YANG Ze-ping, ZHAO Yuan, et al. GUO Yi-xuan, ZHAO Xiu-lan CAO Liu, YANG Jun-xing, GUO Jin-jun, et al. LIN Xiao-bing, ZHOU Li-jun, WANG Hui-ming, et al.	(5108) (5116) (5127) (5135) (5142) (5151) (5163) (5170) (5180) (5189) (5198)
Determination of Heavy Metal Baseline Values and Analysis of Its Accumulation Characteristics in Agricultural Land in Chongqing Characteristics of Organochlorine Pesticides (OCPs) in Soil Samples of Hanjiang River Basin, Southeast China Occurrence and Distribution of the Organophosphate Esters in Soils of Mixed-land Use Area in Chongqing City Degradation of α -HCH in Soil Washing Solutions with nZVI and CaO $_2$ Microbial Communities in Soils of Qingshuitang Industrial District in Zhuzhou Effect of Biochar Addition on the Diversity and Interaction of Rhizosphere Fungi in Manure-fertilized Soil Effects of Returning Nitrogen by Biochar Loading on Paddy Growth, Root Morphology, and Nitrogen Use Efficiency Effect of Particulate Organic Matter on Cadmium Uptake and Transport in Rice Effect of Fertilizers on Cadmium Uptake and Accumulation by Sunflowers	s FANG Ping, TANG An-ping, FU Xing-min, et al. WU Fu-lin, CHEN Li, YI Ting-hui, et al. LIU Jia, DING Yang, QI Shi-hua, et al. YANG Zhi-hao, HE Ming-jing, YANG Ting, et al. YAO Jing-bo, ZHOU Jie, WANG Ming-xin, et al. SHEN Li, LI Zhen-hua, ZENG Wei-min, et al. WANG Dan-dan, YANG Ze-ping, ZHAO Yuan, et al. GUO Yi-xuan, ZHAO Xiu-lan CAO Liu, YANG Jun-xing, GUO Jin-jun, et al. LIN Xiao-bing, ZHOU Li-jun, WANG Hui-ming, et al.	(5108) (5116) (5127) (5135) (5142) (5151) (5163) (5170) (5180) (5189) (5198)
Determination of Heavy Metal Baseline Values and Analysis of Its Accumulation Characteristics in Agricultural Land in Chongqing Characteristics of Organochlorine Pesticides (OCPs) in Soil Samples of Hanjiang River Basin, Southeast China Occurrence and Distribution of the Organophosphate Esters in Soils of Mixed-land Use Area in Chongqing City Degradation of α -HCH in Soil Washing Solutions with nZVI and CaO ₂ Microbial Communities in Soils of Qingshuitang Industrial District in Zhuzhou Effect of Biochar Addition on the Diversity and Interaction of Rhizosphere Fungi in Manure-fertilized Soil Effects of Returning Nitrogen by Biochar Loading on Paddy Growth, Root Morphology, and Nitrogen Use Efficiency Effect of Particulate Organic Matter on Cadmium Uptake and Transport in Rice Effect of Fertilizers on Cadmium Uptake and Accumulation by Sunflowers Accumulation of Heavy Metals in Different Rice Varieties Intercropping Arundo donax with Woody Plants to Remediate Heavy Metal-Contaminated Soil Daily Variation of CO ₂ Flux at Water-Air Interface and Analysis of Its Affecting Factors in a Typical River of the Three Gorges Ro	s FANG Ping, TANG An-ping, FU Xing-min, et al. WU Fu-lin, CHEN Li, YI Ting-hui, et al. LIU Jia, DING Yang, QI Shi-hua, et al. YANG Zhi-hao, HE Ming-jing, YANG Ting, et al. YAO Jing-bo, ZHOU Jie, WANG Ming-xin, et al. SHEN Li, LI Zhen-hua, ZENG Wei-min, et al. WANG Dan-dan, YANG Ze-ping, ZHAO Yuan, et al. YU Ying-liang, WANG Yue-man, HOU Peng-fu, et al. CAO Liu, YANG Jun-xing, GUO Jin-jun, et al. LIN Xiao-bing, ZHOU Li-jun, WANG Hui-ming, et al. ZENG Peng, GUO Zhao-hui, XIAO Xi-yuan, et al. Seservoir LUO Jia-chen, LI Si-yue	(5108) (5116) (5127) (5135) (5142) (5151) (5163) (5170) (5180) (5189) (5198) (5207) (5217)
Determination of Heavy Metal Baseline Values and Analysis of Its Accumulation Characteristics in Agricultural Land in Chongqing Characteristics of Organochlorine Pesticides (OCPs) in Soil Samples of Hanjiang River Basin, Southeast China Occurrence and Distribution of the Organophosphate Esters in Soils of Mixed-land Use Area in Chongqing City Degradation of α -HCH in Soil Washing Solutions with nZVI and CaO ₂ Microbial Communities in Soils of Qingshuitang Industrial District in Zhuzhou Effect of Biochar Addition on the Diversity and Interaction of Rhizosphere Fungi in Manure-fertilized Soil Effects of Returning Nitrogen by Biochar Loading on Paddy Growth, Root Morphology, and Nitrogen Use Efficiency Effect of Particulate Organic Matter on Cadmium Uptake and Transport in Rice Effect of Fertilizers on Cadmium Uptake and Accumulation by Sunflowers Accumulation of Heavy Metals in Different Rice Varieties Intercropping Arundo donax with Woody Plants to Remediate Heavy Metal-Contaminated Soil	s FANG Ping, TANG An-ping, FU Xing-min, et al. WU Fu-lin, CHEN Li, YI Ting-hui, et al. LIU Jia, DING Yang, QI Shi-hua, et al. YANG Zhi-hao, HE Ming-jing, YANG Ting, et al. YAO Jing-bo, ZHOU Jie, WANG Ming-xin, et al. SHEN Li, LI Zhen-hua, ZENG Wei-min, et al. WANG Dan-dan, YANG Ze-ping, ZHAO Yuan, et al. YU Ying-liang, WANG Yue-man, HOU Peng-fu, et al. CAO Liu, YANG Jun-xing, GUO Jin-jun, et al. LIN Xiao-bing, ZHOU Li-jun, WANG Hui-ming, et al. ZENG Peng, GUO Zhao-hui, XIAO Xi-yuan, et al. Seservoir LUO Jia-chen, LI Si-yue	(5108) (5116) (5127) (5135) (5142) (5151) (5163) (5170) (5180) (5189) (5198) (5207) (5217)
Determination of Heavy Metal Baseline Values and Analysis of Its Accumulation Characteristics in Agricultural Land in Chongqing Characteristics of Organochlorine Pesticides (OCPs) in Soil Samples of Hanjiang River Basin, Southeast China Occurrence and Distribution of the Organophosphate Esters in Soils of Mixed-land Use Area in Chongqing City Degradation of α -HCH in Soil Washing Solutions with nZVI and CaO ₂ Microbial Communities in Soils of Qingshuitang Industrial District in Zhuzhou Effect of Biochar Addition on the Diversity and Interaction of Rhizosphere Fungi in Manure-fertilized Soil Effects of Returning Nitrogen by Biochar Loading on Paddy Growth, Root Morphology, and Nitrogen Use Efficiency Effect of Particulate Organic Matter on Cadmium Uptake and Transport in Rice Effect of Fertilizers on Cadmium Uptake and Accumulation by Sunflowers Accumulation of Heavy Metals in Different Rice Varieties Intercropping Arundo donax with Woody Plants to Remediate Heavy Metal-Contaminated Soil Daily Variation of CO ₂ Flux at Water-Air Interface and Analysis of Its Affecting Factors in a Typical River of the Three Gorges Ro	s FANG Ping, TANG An-ping, FU Xing-min, et al. g	(5108) (5116) (5127) (5135) (5142) (5151) (5163) (5170) (5180) (5189) (5198) (5207) (5217) (5227)
Determination of Heavy Metal Baseline Values and Analysis of Its Accumulation Characteristics in Agricultural Land in Chongqing Characteristics of Organochlorine Pesticides (OCPs) in Soil Samples of Hanjiang River Basin, Southeast China Occurrence and Distribution of the Organophosphate Esters in Soils of Mixed-land Use Area in Chongqing City Degradation of α-HCH in Soil Washing Solutions with nZVI and CaO₂ Microbial Communities in Soils of Qingshuitang Industrial District in Zhuzhou Effect of Biochar Addition on the Diversity and Interaction of Rhizosphere Fungi in Manure-fertilized Soil Effects of Returning Nitrogen by Biochar Loading on Paddy Growth, Root Morphology, and Nitrogen Use Efficiency Effect of Particulate Organic Matter on Cadmium Uptake and Transport in Rice Effect of Fertilizers on Cadmium Uptake and Accumulation by Sunflowers Accumulation of Heavy Metals in Different Rice Varieties Intercropping Arundo donax with Woody Plants to Remediate Heavy Metal-Contaminated Soil Daily Variation of CO₂ Flux at Water-Air Interface and Analysis of Its Affecting Factors in a Typical River of the Three Gorges Ro CH₄ Emissions Characteristics and Its Influencing Factors in an Eutrophic Lake Short-term Effects of Different Grazing Intensities on Greenhouse Gas Fluxes in Semi-arid Grassland Effects of Plastic Film Mulching Patterns and Irrigation on Yield of Summer Maize and Greenhouse Gas Emissions Intensity of Fie	s FANG Ping, TANG An-ping, FU Xing-min, et al. g	(5108) (5116) (5117) (5135) (5142) (5151) (5163) (5170) (5180) (5189) (5207) (5207) (5217) (5227) (5237) (5246)
Determination of Heavy Metal Baseline Values and Analysis of Its Accumulation Characteristics in Agricultural Land in Chongqing Characteristics of Organochlorine Pesticides (OCPs) in Soil Samples of Hanjiang River Basin, Southeast China Occurrence and Distribution of the Organophosphate Esters in Soils of Mixed-land Use Area in Chongqing City Degradation of α-HCH in Soil Washing Solutions with nZVI and CaO ₂ Microbial Communities in Soils of Qingshuitang Industrial District in Zhuzhou Effect of Biochar Addition on the Diversity and Interaction of Rhizosphere Fungi in Manure-fertilized Soil Effects of Returning Nitrogen by Biochar Loading on Paddy Growth, Root Morphology, and Nitrogen Use Efficiency Effect of Particulate Organic Matter on Cadmium Uptake and Transport in Rice Effect of Fertilizers on Cadmium Uptake and Accumulation by Sunflowers Accumulation of Heavy Metals in Different Rice Varieties Intercropping Arundo donax with Woody Plants to Remediate Heavy Metal-Contaminated Soil Daily Variation of CO ₂ Flux at Water-Air Interface and Analysis of Its Affecting Factors in a Typical River of the Three Gorges Ro CH ₄ Emissions Characteristics and Its Influencing Factors in an Eutrophic Lake Short-term Effects of Different Grazing Intensities on Greenhouse Gas Fluxes in Semi-arid Grassland	s FANG Ping, TANG An-ping, FU Xing-min, et al. g	(5108) (5116) (5117) (5135) (5142) (5151) (5163) (5170) (5180) (5189) (5207) (5207) (5217) (5227) (5237) (5246)
Determination of Heavy Metal Baseline Values and Analysis of Its Accumulation Characteristics in Agricultural Land in Chongqing Characteristics of Organochlorine Pesticides (OCPs) in Soil Samples of Hanjiang River Basin, Southeast China Occurrence and Distribution of the Organophosphate Esters in Soils of Mixed-land Use Area in Chongqing City Degradation of α-HCH in Soil Washing Solutions with nZVI and CaO₂ Microbial Communities in Soils of Qingshuitang Industrial District in Zhuzhou Effect of Biochar Addition on the Diversity and Interaction of Rhizosphere Fungi in Manure-fertilized Soil Effects of Returning Nitrogen by Biochar Loading on Paddy Growth, Root Morphology, and Nitrogen Use Efficiency Effect of Particulate Organic Matter on Cadmium Uptake and Transport in Rice Effect of Fertilizers on Cadmium Uptake and Accumulation by Sunflowers Accumulation of Heavy Metals in Different Rice Varieties Intercropping Arundo donax with Woody Plants to Remediate Heavy Metal-Contaminated Soil Daily Variation of CO₂ Flux at Water-Air Interface and Analysis of Its Affecting Factors in a Typical River of the Three Gorges Ro CH₄ Emissions Characteristics and Its Influencing Factors in an Eutrophic Lake Short-term Effects of Different Grazing Intensities on Greenhouse Gas Fluxes in Semi-arid Grassland Effects of Plastic Film Mulching Patterns and Irrigation on Yield of Summer Maize and Greenhouse Gas Emissions Intensity of Fie	s FANG Ping, TANG An-ping, FU Xing-min, et al. WU Fu-lin, CHEN Li, YI Ting-hui, et al. LIU Jia, DING Yang, QI Shi-hua, et al. YANG Zhi-hao, HE Ming-jing, YANG Ting, et al. YAO Jing-bo, ZHOU Jie, WANG Ming-xin, et al. SHEN Li, LI Zhen-hua, ZENG Wei-min, et al. WANG Dan-dan, YANG Ze-ping, ZHAO Yuan, et al. GUO Yi-xuan, ZHAO Xiu-lan CAO Liu, YANG Jun-xing, GUO Jin-jun, et al. LIN Xiao-bing, ZHOU Li-jun, WANG Hui-ming, et al. ZENG Peng, GUO Zhao-hui, XIAO Xi-yuan, et al. SHANG Dong-yao, XIAO Qi-tao, HU Zheng-hua, et al. SHEN Yan, SUN Jian-ping, LUO Yu-kun, et al. SHEN Yan, SUN Jian-ping, LUO Yu-kun, et al. TENG Zhao-zhong, YUAN Xiang-yang	(5108) (5116) (5127) (5135) (5142) (5151) (5163) (5170) (5180) (5189) (5207) (5217) (5227) (5227) (5237) (5246) (5257)